Mechanical, Morphological and Chemical properties of Bio-degradable Nanocomposite Poly- Lactic acid/ TiO_2

[1]Kanchan Arvind Ingle, [2]Prof.Dr.G.S.Zamre, [3]Prof. Dr.P.V.Thorat

[1]Student, [2]Professor, [3]Head of Department
Department of Chemical Engineering,
College of Engineering & Technology, Akola, Maharashtra, India

***Abstract*: Bionanocomposites from biopolymers and inorganic nanoparticles are of great interest for packaging materials due to their enhanced physical, thermal, mechanical, and processing characteristics. In this study, poly(lactic acid) (PLA) nanocomposites with bonding between TiO_2 nanowire surface and PLA chains were synthesized through *in situ* melt polycondensation. Molecular weight, structure, morphology, and thermal properties were characterized. Fourier transform infrared spectroscopy confirmed that PLA chains were covalently grafted onto TiO_2 nanowire surface.**

***Index Terms*: Bionanocomposites, Nanowires, Crystallization.**

I. INTRODUCTION

Packaging has been one of the rapidly growing areas for the use of plastics. Out of total plastics production, 41% are used in packaging industry, and 47% are used for food packaging, which are mainly short-term and single use items. The currently used plastics are mainly made from petroleum based polymers, of which the major concerns are their issues of being non-biodegradable and having non-renewable sources.

Poly (lactic acid) (PLA), derived from renewable sugar based resources (starch, sugar cane, cellulose, etc.), has shown great potential as a biodegradable packaging plastic. However, the low glass transition/heat distortion temperatures around 60 ºC and slow biodegradation rate have severely limited its broad disposable applications.

Toyota researchers in the early 1990s who added 4.7% nano-clay into nylon 6 resulting in about 50% increase in the strength/modulus and 87 ºC increase in the heat distortion temperature, synthesizing polymer nanocomposites (PNCs) offers a new approach to enhancing the physical, thermal, and mechanical properties of polymers. PLA nanocomposites have been reported using various nanoparticles, including carbon nanotubes, layered silicates or clays, silica, graphite, polyhedral oligomeric silsesquioxane, magnesium oxide, etc.. Though those nanocomposites exhibited enhanced mechanical strength, very few nanoparticles could efficiently improve the glass transition temperature (T_g) and degradation rate of PLA because of the lack of strong interfacial interactions between nanoparticles and PLA matrix and the lack of effective degradation promoters.

Because of the capability of absorbing UV light ($\lambda < 388$ nm) to generate oxygen species, TiO_2 nanoparticles have been applied to promote the photodegradation of various organic chemicals such as aldehyde, toluene, and benzene. Once TiO_2 nanoparticles are incorporated into polymer matrix, these active oxygen species will lead to photodegradation reaction by attacking the interfacial polymer chains, forming carbon-centered radicals, and accelerating chain cleavage. Incorporated TiO_2 nanoparticles into PE and PS, and they reported significant photodegradation of polymer matrix after UV irradiation for a period of time. Although biodegradation of PLA can be advanced in the ground with appropriate moisture and bacteria, it still requires a long period of time, and this biodegradation does not advance in the air. By adding photosensitive TiO_2 nanoparticles into biodegradable PLA, PLA nanocomposites can possess both photodegradability and biodegradability, and thus the degradation can be promoted under any conditions. Recent advances make it possible to synthesize considerable quantities of TiO_2 nanowires. The extended nanoparticles (i.e., nanowires) can more easily form network structures through either direct interaction between the nanoparticles or chain bridging between the nanoparticles, which is believed to play a significant role in property enhancement, compared with conventional nanospheres. Furthermore, large quantities of hydroxyl groups on the TiO_2 nanoparticle surface enable it to be functionalized with organic monomers or grafted with polymer chains.

The two challenges of synthesizing PNCs with targeted properties are the difficulties in achieving nanoscale homogeneous dispersion and strong interfacial interaction between nanoparticles and polymer matrix because nanoparticles typically agglomerate due to their hydrophilic nature and high surface area, and they are not miscible with hydrophobic polymer phase. In order to solve these problems, we first dispersed TiO_2 nanowires into hydrophilic lactic acid with the mechanical stirring. The polymer chains continue growing on the nanowire surface with removal of resultant water during condensation polymerization (as illustrated in Figure 5.1).

The specific objectives of this study are to

(1) synthesize PLA/TiO_2 nanowire nanocomposites via *in situ* melt polycondensation from lactic acid with different TiO_2 nanowire loadings;

(2) characterize the properties of PLA- TiO_2 (PLA--TiO_2) nanowires isolated from free PLA in the PLA/2%TiO_2 nanowire bulk nanocomposites to confirm the surface polymerization; and

(3) characterize the molecular weight, structure, morphology, and thermal properties of the bulk nanocomposites.

II. EXPERIMENTAL SECTION- NANOWIRE PREPARATION

For a typical preparation, 0.1 g TiO_2 nanopowders were taken. It was then filled with 40 ml 10 M NaOH aqueous solution, sealed into a stainless steel tank and maintained at 200 ºC for 24h without stirring. After cooling down, the sample was washed with 1

M aqueous HCl solution, deionized water, and absolute ethanol several times and dried at 80 ºC for 12 h. Finally, we obtained soft fibrous TiO_2 nanowires with white color.

POLYMERIZATION:

After cooling down, the oligomer from the previous step was mixed with $SnCl_2{\cdot}H_2O$ (0.4% wt relative to oligomer) and TSA (an equimolar ratio to $SnCl_2{\cdot}H_2O$) as a binary catalyst . The mixture was gradually heated to 180 °C with stirring speed of 200 rpm. The pressure was reduced gradually to 10 torr in 1.5 h. Then the reaction was continued at 180 °C/10 torr for 10 h with stirring speed of 150 rpm. At the end of the reaction, the flask was cooled, and the product was dissolved in chloroform and subsequently precipitated into methanol. The resulting solid was washed with methanol three times and dried under vacuum at 80 ºC for 24 h. Bulk nanocomposites were labeled according to the concentrations of TiO_2 nanowires as PLA/0.25%TiO_2, PLA/0.5%TiO_2, PLA/1%TiO_2, and PLA/2%TiO_2. Pure PLA without TiO_2 nanowires was prepared following the same procedures and used as a control.

III. RESULTS AND DISCUSSION

SYNTHESIZED TiO_2 NANOWIRES

Powder X-ray diffraction indicated that the TiO_2 nanowires were dominated by crystal structure. The UV-vis spectrum indicated that the TiO_2 nanowires had a strong UV absorption ability with absorption peak at 294 nm (Figure 5.2). The threshold of UV absorption is ~380 nm, with the energy slightly higher than the bandgap of bulk TiO_2 crystals

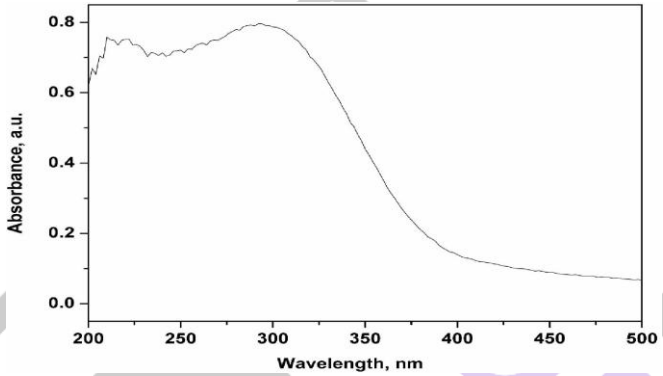

Figure 5.2 UV-vis spectrum of pristine TiO_2 nanowires.

.

MOLECULAR WEIGHT

Molecular weight and PDI of PLA and PLA/TiO_2 nanowire bulk nanocomposites are listed in Table 5.1. The M_w and M_n of pure PLA were 63,000 and 33,500, respectively, with PDI of 1.9. The M_n of bulk nanocomposites with 0.25% TiO_2 nanowires was increased by 12% compared with pure PLA, with a broader PDI of 2.2. Similar molecular weight values to pure PLA were obtained for bulk nanocomposites with 0.5 and 1% TiO_2 nanowires.

PLA/2%TiO_2 bulk nanocomposites showed significantly increased molecular weight, with M_w and M_n increased by 66 and 65%, respectively, compared with those of pure PLA. A similar increment of molecular weight was obtained for free PLA, which was isolated from PLA/2%TiO_2 bulk nanocomposites. As observed under TEM (not shown), quite a lot TiO_2 nanowires were noticed in free PLA, indicating that some TiO_2 nanowires were dispersed into chloroform during the centrifugation process. The increase of molecular weight might be explained by two reasons. First, although the nanocomposite solution was filtered with filter before GPC measurement, some nanowires could still pass the filter due to the significantly decreased size, as will be discussed in the morphology section, contributing to the higher molecular hydrodynamic volume. Second, the grafted PLA chains on the nanowire surface formed polymer brushes (Figure 5.1), which also resulted in increased molecular weight.

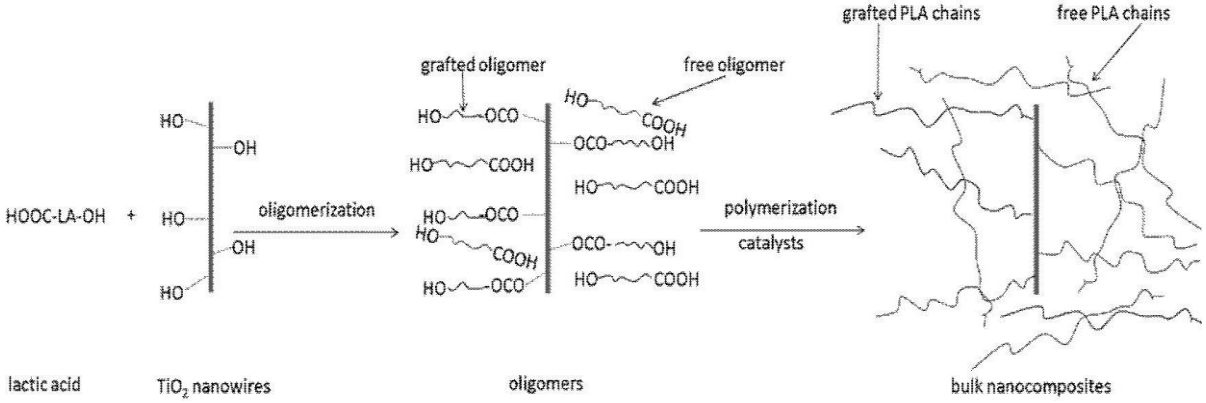

Figure 5.1 Illustration of the synthesis approach for PLA/TiO_2 nanowire nanocomposites.

I. Table 5.1 Molecular weight of PLA and bulk nanocomposites containing TiO_2 nanowires determined by GPC measurement

Sample	M_w	M_n	[a]PDI

PLA	63,000	33,500	1.9
PLA-0.25%TiO_2	83,300	37,500	2.2
PLA-0.5% TiO_2	66,800	34,500	1.9
PLA-1% TiO_2	66,100	31,300	2.1
PLA-2% TiO_2	104,800	55,200	1.9
free PLA	104,300	59,200	1.8

PDI –Molecular weight distribution (M_w/ M_n)

FTIR

The FTIR spectra of PLA, pristine TiO_2 nanowires, PLA-TiO_2 nanowires, and PLA/2% TiO_2 nanowire bulk nanocomposites before isolating are presented in Figure 5.3. Pristine TiO_2 nanowires showed bands around 3200 and 1640 cm^{-1}, corresponding to the stretching and bending vibrations of hydroxyl groups on the TiO_2 nanowire surface. The strong absorption band between 1000 and 400 cm^{-1} were attributed to the Ti-O and Ti-O-Ti vibrations. PLA showed strong C=O stretching band at 1758 cm^{-1}, and C-O stretching band at 1182, 1128, and 1090 cm^{-1}. The asymmetric and symmetric stretching bands of C-H from CH_3 groups of the side chains were observed at 2996 and 2878 cm^{-1}, whereas their bending vibration was observed at 1455 cm^{-1}. The band at 2946 cm^{-1} was attributed to the stretching of C-H groups in the main chain of PLA, and its bending vibrations appeared at 1384 and 1358 cm^{-1}. After formation of TiO_2 nanowires, the bands at 1756, 1184, 1130, 1090 cm^{-1} were caused by the vibrations of C=O and C-O groups from grafted PLA chains. Besides, new bands appeared at 1554 and 1421 cm^{-1} due to the bidentate coordination between Ti atoms and the carboxylic groups of lactic acid. FTIR results indicated that PLA chains were successfully grafted onto TiO_2 nanowire surface. PLA/TiO_2 nanowire bulk nanocomposites showed similar spectra as pure PLA, and the typical spectrum of nanocomposites containing 2% TiO_2 nanowires was presented in Figure 5.3. We did not observe the Ti-O band for the bulk nanocomposites because of the relatively low concentrations of TiO_2 nanowires.

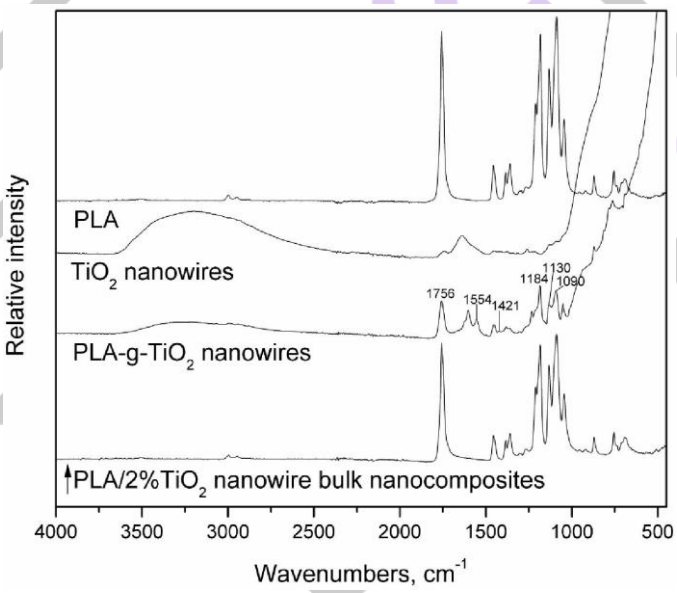

Figure 5.3 FTIR spectra of PLA, pristine TiO_2 nanowires,and PLA/2% TiO_2 nanowire bulk nanocomposites.

MORPHOLOGY

Figure 5.4 illustrated the SEM micrographs of pristine TiO_2 nanowires and PLA- TiO_2 nanowires. The nanowires exhibited quite clean surface. The diameter was ~50- 200 nm and length from a few micrometers to ~20 micrometers (Figure 5.4A), which is consistent with the literature. The pristine nanowires were aggregated but were still as single wires at higher magnification. Such nanowires were easily dispersed into lactic acid monomer homogeneously at the beginning of polymerization.

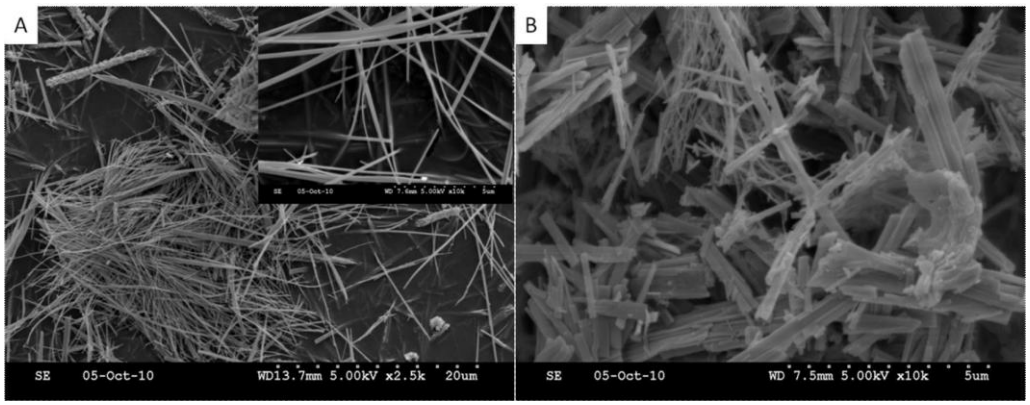

Figure 5.4 SEM micrographs of (A) pristine TiO_2 nanowires and (B) PLA-TiO_2 nanowires (scale bar is indicated at the bottom of each image)

As an additional evidence for the existence of PLA chains on nanowire surface, analysis of TEM was conducted and the typical results are shown in Figure 5.5. Similar to SEM, significant reduction of size was also noticed for PLA-TiO_2 nanowires under TEM, compared with that ofTiO_2 nanowires (Figure 5.5A and B). The surface of TiO_2 nanowires seemed to be smooth and clear without any extra phase adhering to them (Figure 5.5A'). In contrast, the PLA-TiO_2 nanowires shown in Figure 5.5B' appeared stained with extra phase (dark area on the nanowire surface) that is presumed to come from grafted PLA molecules.

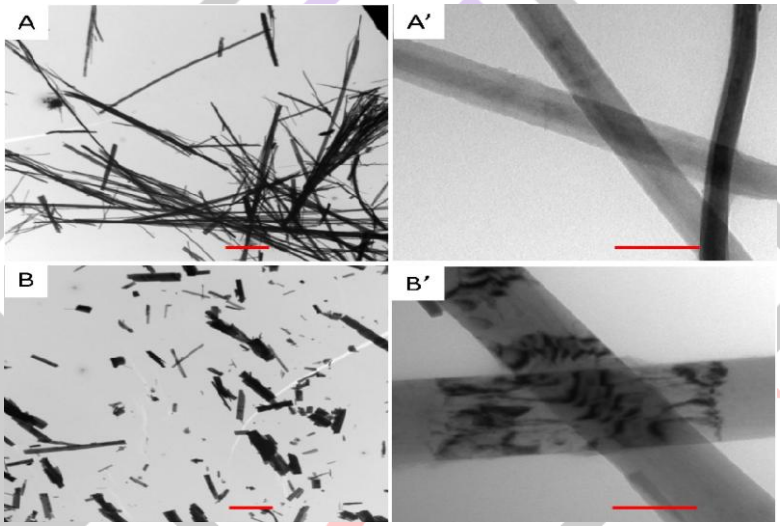

Figure 5.5 TEM micrographs of (A and A') synthesized TiO_2 nanowires and (B and B') PLA-TiO_2 nanowires (scale bar: left, 2 µm; right, 100 nm).

The SEM micrographs of PLA and bulk nanocomposites are presented in Figure 5.6.
The surface of pure PLA was quite flat and smooth (Figure 5.6a). As the concentration of TiO_2 nanowires increased, much more coarse and uneven surfaces were observed for the bulk nanocomposites (Figure 5.6b-e) and did not observe any phase separation in the bulk nanocomposites.

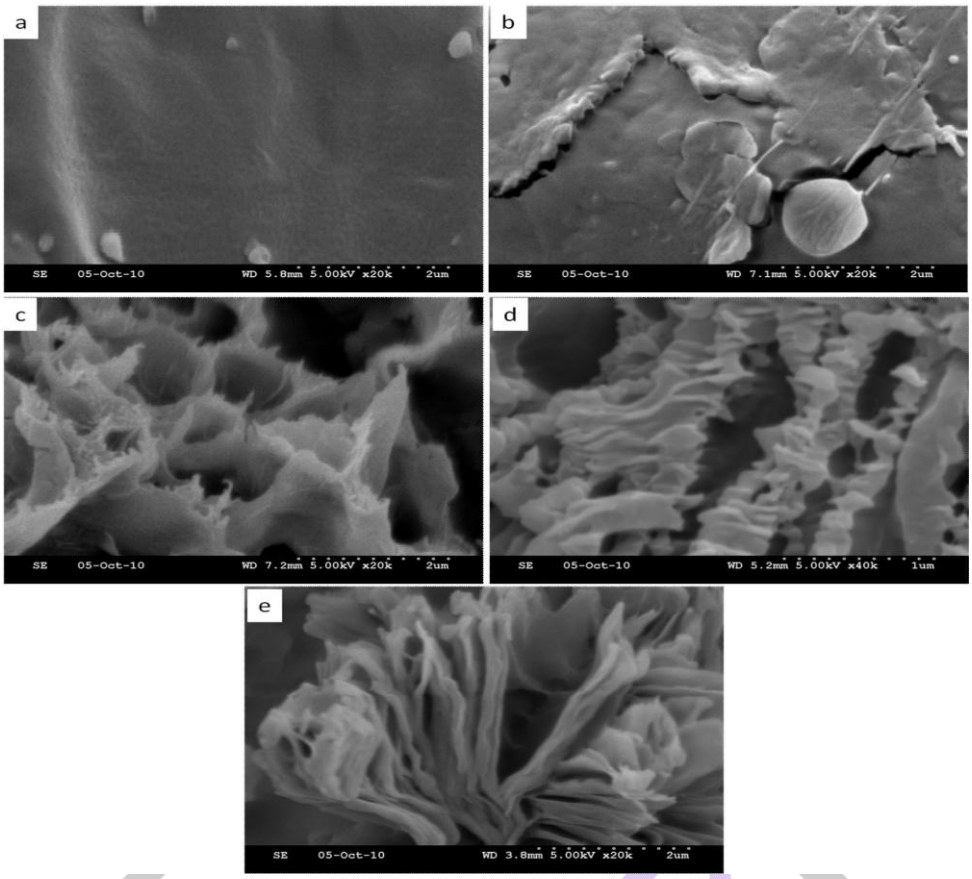

Figure 5.6 SEM micrographs of PLA/TiO_2 nanowire bulk nanocomposites (a, PLA; b, PLA/0.25%TiO_2; c, PLA/0.5%TiO_2; d, PLA/1%TiO_2; e, PLA/2%TiO_2; scale bar is indicated at the bottom of each image).

TEM is a powerful tool for studying the dispersion of nanoparticles embedded within a polymer matrix. The typical TEM micrographs of PLA and bulk nanocomposites are shown in Figure 5.7. No nanowire aggregation was observed in the polymer matrix. The individual nanowires appeared to be distributed homogeneously throughout the polymer matrix (Figure 5.7c/c'). At higher magnification, we observed that the nanowire surface was covered with a third phase due to the presence of PLA (inserted image of Figure 5.7c'). TEM images indicated that the distinct phase on TiO_2 nanowire surfaces prevented the hydrophilic aggregation of nanowires and resulted in a better dispersion of nanowires. It could also improve the hydrophobic entanglements of PLA chains with surrounding free PLA matrix.

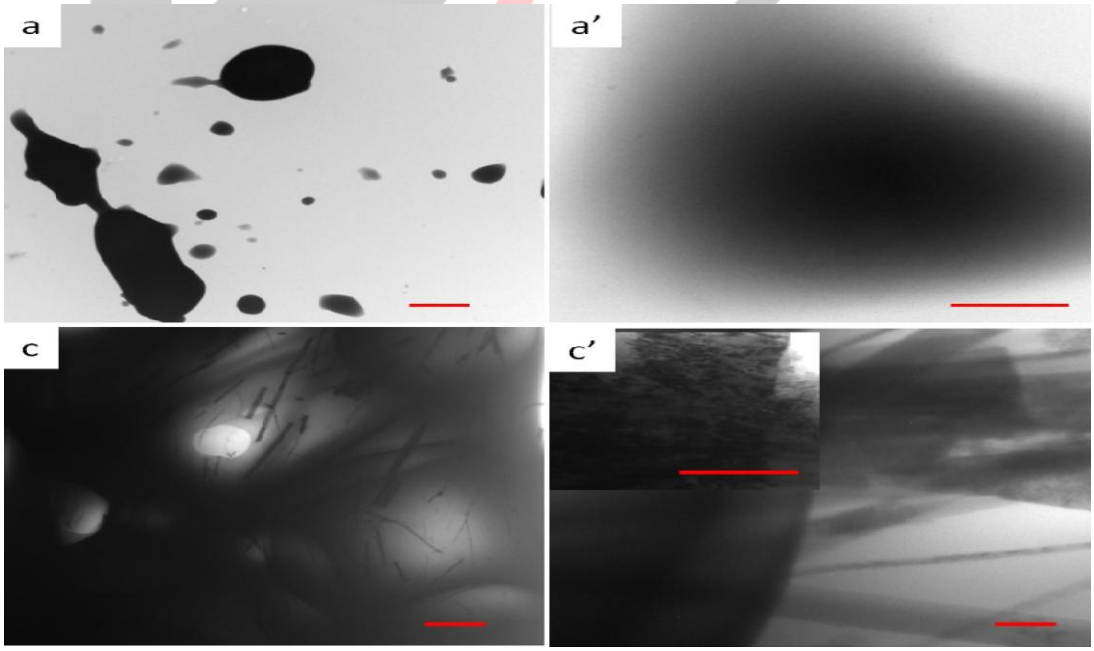

Figure 5.7 Typical TEM micrographs of PLA and PLA/TiO_2 nanowire bulk nanocomposites (a/a', PLA; c/c', PLA/0.5%TiO_2; scale bar: left, 2 µm; right, 200 nm).

THERMAL PROPERTIES

DSC thermograms showing the T_g of pure PLA and PLA-TiO_2 nanowires are presented in Figure 5.8. The T_g was determined from the half width midpoint between the onset and the end temperatures of the transition, as indicated by the dash lines in the thermograms. About a 7 ºC increment of T_g was observed for those PLA chains onto TiO_2 nanowire surface compared with pure PLA, as obtained from the first DSC heating scan (Figure 5.8A). After erasing the thermal history, although the T_g of both PLA and PLA- TiO_2 nanowires decreased due to the loss of the chain conformational ordering, T_g of the latter was still 6 ºC higher (Figure 5.8B). The very small heat capacity change at the glass transition for PLA-TiO_2 nanowires was probably because of the low PLA ratios (~ 30%) in the sample and relatively short PLA chains. The increased T_g sustained the evidence that strong bonding exited between the PLA chains and TiO_2 nanowires, which led to permanent attachment of PLA chain segments onto the TiO_2 nanowire surface. The increased T_g was caused by the restrictions on the mobility of chains in the vicinity of the surface. The reduction of chain mobility was possibly caused by crowding and/or local ordering of chains at the interface as well as loss of configurational entropy of the PLA segments near the nanowire surface . Molecular dynamics simulations also showed that the relaxations of chain segments in the immediate vicinity of the nanoparticles were slower.

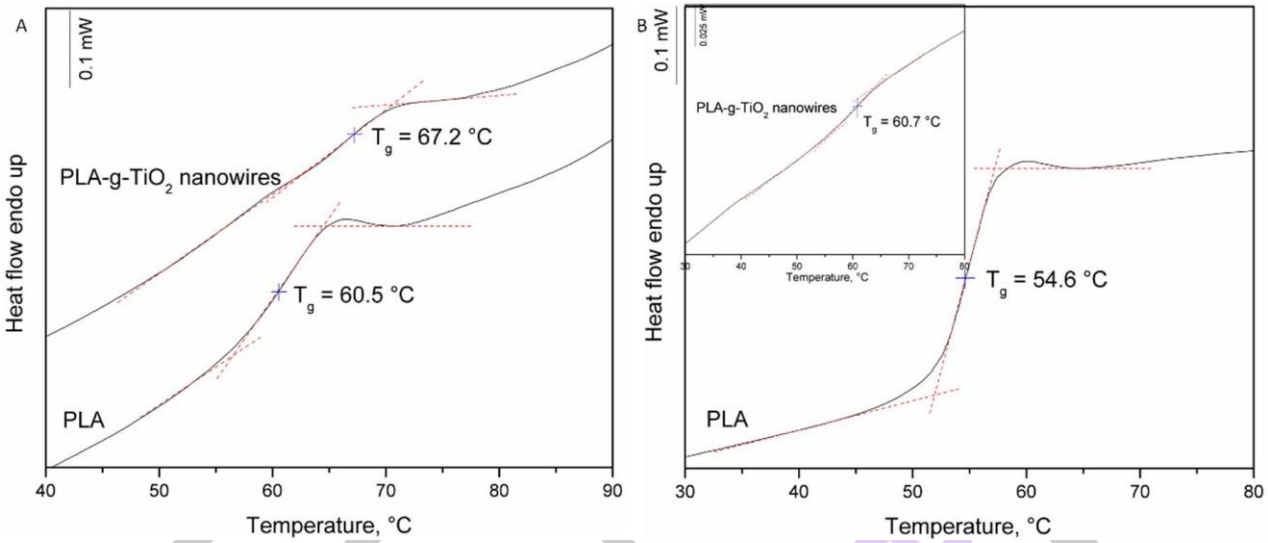

Figure 5.8 DSC thermograms of PLA and PLA--TiO_2 nanowires (A, first heating scan; B, second heating scan).

Figure 5.9 shows the DSC thermograms of PLA/TiO_2 nanowire bulk nanocomposites, and quantified results are summarized in Table 5.2. All the thermograms were obtained from the second DSC heating scan after erasing the thermal history, and they exhibited three thermal transitions, i.e., glass transition, cold crystallization, and melting of PLA. Pure PLA showed a T_g of 54.7 ºC, while the bulk nanocomposites exhibited elevated T_g as the TiO_2 nanowire concentrations were increased from 0 to 2%. Maximum T_g was obtained for PLA/2%TiO_2 nanowire bulk nanocomposites, which was 4 ºC higher than that of pure PLA. As discussed before, the permanent graft of PLA chains onto the nanowire surface leads to restricted mobility of chain segments; therefore, T_g increased. With higher concentrations of nanowires in bulk nanocomposites, more grafted chain segments onto nanowire surface were expected, leading to larger T_g.

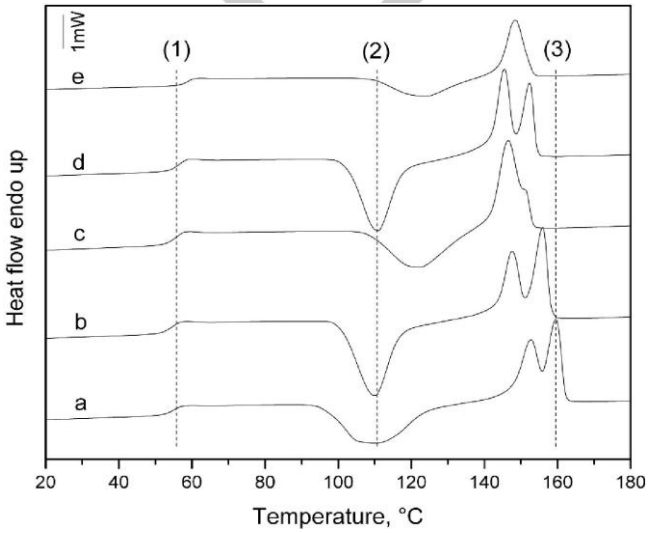

Figure 5.9 DSC thermograms of PLA/TiO_2 nanowire bulk nanocomposites (a, PLA; b, PLA/0.25%TiO_2; c, PLA/0.5%TiO_2; d, PLA/1%TiO_2; e, PLA/2%TiO_2). (1) Glasstransition, (2) cold crystallization, and (3) melting

Sample	Tg°C	ΔC_p J/(g·°C)	T_c °C	ΔH_c J/g	T_m °C	ΔH_m J/g	X_m %
PLA	54.7	0.55	110.0	43.1	152.7, 159.5	43.5	46.5
PLA-0.25%TiO_2	54.9	0.52	110.1	36.5	147.6, 155.9	36.9	39.5
PLA-0.5% TiO_2	55.1	0.55	122.1	25.8	146.5, 151.0	26.8	28.8
PLA-1% TiO_2	56.2	0.49	110.8	34.0	145.5, 152.2	35.1	37.9
PLA-2% TiO_2	58.4	0.50	123..7	21.4	148.5	24.5	26.7

Table 5.2 Thermal properties of PLA and bulk nanocomposites containing TiO_2 nanowires determined from DSC thermograms

The T_c and T_m of pure PLA was 110 and 153/160 °C, respectively, with crystallinity of 47%. Decreased crystallinity was observed for all the bulk nanocomposites with TiO_2 nanowires. Bulk nanocomposites with 0.5 and 2% nanowires exhibited lowest crystallinity. More than a 10 °C increment of T_c was observed for these two bulk nanocomposites, implying their lowest crystallization ability. These phenomena were probably caused by the reduction of the diffusion of the PLA chains to the growing crystalline lamella and disruption of the regularity of the chain structures in PLA in the presence of TiO_2 nanowires. The incontinuous decrease of crystallinity with increasing nanowire loadings might be related with an inhomogeneous dispersion of TiO_2 nanowires in samples with the lowest crystallinity, and improved nanowire dispersion for the other ones. PLA and bulk nanocomposites with less than 1% TiO_2 nanowires exhibited double melting behaviors, which were caused by the separate melting of the PLA crystals with low structural perfection and normal PLA crystals and the melting-recrystallization to the higher perfection-remelting process of PLA crystals. Decreased T_m was obtained for bulk nanocomposites with increased concentration of TiO_2 nanowires. Double melting peaks merged into one single peak at 149 °C for PLA/2%TiO_2 nanowire bulk nanocomposites, indicating the difficulties in forming PLA crystals with higher perfection at high concentration of nanowires, which might be caused the presence of more grafted PLA chains.

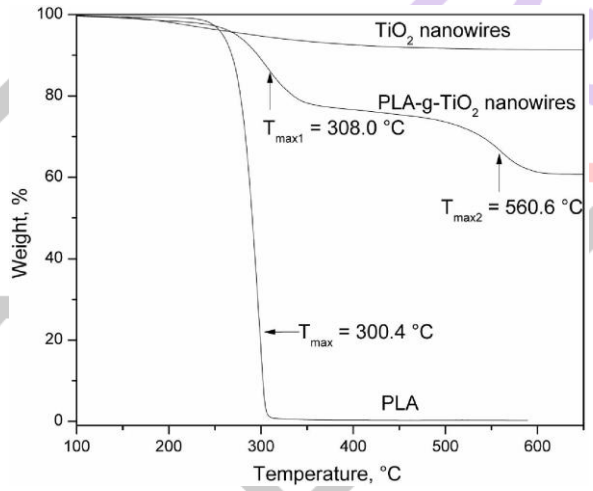

Figure 5.10 TGA thermograms of PLA, pristine TiO_2 nanowires, and PLA-g-TiO_2 nanowires under air atmosphere.

The TGA thermograms of intensively dried PLA, pristine TiO_2 nanowires, and PLA-TiO_2 nanowires are presented in Figure 5.10. These thermograms were obtained under air atmosphere to quantitatively estimate ratio of organic PLA chains on the TiO_2 nanowire surface. The weight loss of TiO_2 nanowires and PLA-TiO_2 nanowires were 9 and 40% respectively, after achieving the thermogram plateaus during heating. Based on the differences of weight loss between TiO_2 nanowires before and after surface grafting, more than 30% PLA in weight were certainly grafted onto nanowire surface. The grafted PLA chains exhibited two-stage thermal decomposition behaviors. The first decomposition occurred at the peak temperature of 308 °C, which was related to the polymer chains far away from the nanowire surfaces. The first decomposition temperature was slightly higher than that of pure PLA (300 °C). The second decomposition occurred at the peak temperature of 560 °C, which was probably caused by the polymer chains in the vicinity of the nanowires.

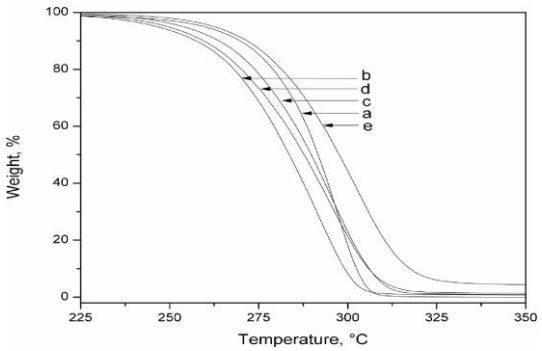

Figure 5.11 TGA thermograms of PLA/TiO_2 nanowire bulk nanocomposites under nitrogen atmosphere (a, PLA; b, PLA/0.25%TiO_2; c,PLA/0.5%TiO_2; d, PLA/1%TiO_2; e, PLA/2%TiO_2).

The thermal stability of PLA and bulk nanocomposites with TiO_2 nanowires was studied via TGA under an inert nitrogen atmosphere. The TGA thermograms are shown in Figure 5.11, and the decomposition data are summarized in Table 5.3. Pure PLA exhibited a peak decomposition temperature (T_{max}) of 297 ºC and onset (T_{onset}) and end (T_{end}) decomposition temperatures of 276 and 308 ºC. Broader decomposition ranges (T_{end} - T_{onset}) were observed for all the bulk nanocomposites, due to their more complex structures (i.e., free PLA chains, grafted chains in the vicinity of nanowire surfaces, grafted chains far away from nanowire surfaces, chains entangled with nanowires, etc.) compared with pure PLA (Figure 5.1). Decreased T_{onset} was obtained for bulk nanocomposites with less than 1% TiO_2 nanowires, which might be caused by the accelerated decomposition of PLA chains with the aid of extra hydroxyl groups from TiO_2 nanowires. PLA/2%TiO_2 nanowire bulk nanocomposites showed highest T_{max} and T_{end} among pure PLA and other bulk nanocomposites. This might be explained by the fact that more grafted PLA chains resulting from higher concentrations of nanowires played a dominant role in enhancing the thermal stability, while the catalytic effect from extra hydroxyl groups played a subordinate role.

Sample	TonsetºC	Tend ºC	Tmax ºC
PLA	276.2	308.3	296.6
PLA-0.25%TiO_2	254.7	306.4	291.3
PLA-0.5% TiO_2	263.4	314.9	295.7
PLA-1% TiO_2	261.9	314.2	295.7
PLA-2% TiO_2	274.5	322.6	302.3

Table 5.3 Thermal decomposition temperatures of PLA and bulk nanocomposites containing TiO_2 nanowires derived from TGA thermograms

Moreover, the high concentration of TiO_2 nanowires could act as a superior insulator and mass transport barrier to the volatile products generated during decomposition. Significantly increased thermal decomposition temperatures were also reported for PLA/multi-walled carbon nanotube nanocomposites (MWNTs) at higher concentrations of MWNTs.

IV. CONCLUSION

Bionanocomposites with covalent bonding between TiO_2 nanowire surface and PLA chains were synthesized through *in situ* melt polycondensation. The covalent grafting of PLA chains onto the nanowire surfaces was confirmed by FTIR spectroscopy and TGA. TEM micrographs and DSC results also sustained the presence of the third phase on the nanowire surfaces. Those PLA on the nanowire surfaces exhibited significantly increased T_g and thermal stability, compared with pure PLA. TGA results also showed that more than 30% of PLA in weight were certainly grafted onto the nanowire surfaces. Increased molecular weight was obtained for PLA/2%TiO_2 nanowire bulk nanocomposites, of which the M_w was 66% higher than that of pure PLA. TEM micrographs indicated that homogeneous dispersion of TiO_2 nanowires in the PLA matrix was achieved. The T_g of bulk nanocomposites increased, whereas the crystallization ability decreased, as the nanowire concentrations increased from 0 to 2%.

REFERENCES

[1] Benabdillah, K. M., Boustta M., Coudane J., &Vert M. (2001). Chap. 14 Can the Glass Transition Temperature of PLA Polymers Be Increased? In Polymers from Renewable Resources: Biopolyesters and Biocatalysis, ed. by Carmen Scholz, Richard A. Gross, ACS publication, pp 200-220.

[2] Bezrodna, T., Puchkovska, G., Shimanovska, V., Chashechnikova, I., Khalyavka, T., & Baran, J. (2003). Pyridine−TiO2 surface interaction as a probe for surface active centers analysis. Appl. Surf. Sci., 214, 222-231.

[3] Blumstein, A. (1965). Polymerization of adsorbed monolayers: II. thermal degradation of the inserted polymers. J. Polym. Sci., A 3, 2665-2673.

[4] Crosbya, A. J., & Lee, J. Y. (2007). Polymer nanocomposites: the "nano" effect on mechanical properties. Polym. Rev., 47, 217-229.

[5] Džunuzović, E., Vodnik, V., Jeremić, K., & Nedeljković J. M. (2009). Thermal properties of PS/TiO2 nanocomposites obtained by in situ bulk radical polymerization of styrene. Mater. Lett., 63, 908-810.

[6] Fischer, E. W., Sterzel, H. J., & Wegner, G. (1973). Investigation of the structure of solution grown crystals of lactide copolymers by means of chemical reactions. Kolloid Z. Z. Polym., 251, 980-990.
[7] Fomin, V. A., & Guzeev, V. V. (2001). Biodegradable polymers, their present state and future aspects. Prog. Rubb. Plastics Tech., 17, 186-204.
[8] Gnanasekaran, D., Madhavan, K., & Reddy, B. S. R. (2009). Developments of polyhedral oligomeric silsesquioxanes (POSS), POSS nanocomposites and their applications: a review. J. Sci. Ind. Res., 68, 437-464.
[9] Gupta, A. P., & Kumar, V. (2007). New emerging trends in synthetic biodegradable polymers – polylactide: a critique. Eur. Polym. J., 43, 4053-4074.
[10] Haque, S., Rehman, I., & Darr, J. A. (2007). Synthesis and characterization of grafted nanohydroxyapatites using functionalized surface agents. Langmuir, 23, 6671-6676.
[11] Hojjati, B., Sui, R., & Charpentier, P. A. (2007) Synthesis of TiO2/PAA nanocomposite by RAFT polymerization. Polymer, 48, 5850-5858.
[12] Li, Y., & Sun, X. S. (2010). Preparation and characterization of polymer−inorganic nanocomposites by in situ melt polycondensation of L-lactic acid and surface- hydroxylated MgO. Biomacromolecules, 11, 1847–1855.
[13] Paul, D. R., & Robeson, L. M. (2008). Polymer nanotechnology: nanocomposites. Polymer, 49, 3187-3204.
[14] Ray, S. S., & Bousmina, M. (2005). Biodegradable polymers and their layered silicate nanocomposites: in greening the 21st century materials world. Prog. Mater. Sci., 50, 962-1079.
[15] Tsuji, H., Kawashima, Y., Takikawa, H., & Tanaka, S. (2007). Poly(l-lactide)/nano- structured carbon composites: conductivity, thermal properties, crystallization, and biodegradation. Polymer, 48, 4213-4225.
[16] Usuki, A., Kojima, Y., Kawasumi, M., Okada, A., Fukushima, Y., Kurauchi, T., & Kamigaito, O. (1993). Synthesis of nylon 6-clay hybrid. J. Mater. Res., 8, 1179-1184.
[17] Wang, B., Sun, X. S., Klabunde, K. J. (2009). Poly(lactic acid)/multi-hydroxyl magnesium oxide nanocomposites prepared by melt compounding. J. Biobased Mater. Bioenergy, 3, 130-138.